Exp Brain Res (2002) 147:145–152
DOI 10.1007/s00221-002-1178-6

RESEARCH ARTICLE

Roman Bauer · Sabine Heinze

Contour integration in striate cortex

Classic cell responses or cooperative selection?

Received: 15 October 2001 / Accepted: 29 May 2002 / Published online: 1 October 2002

Abstract Psychophysics has established various rules of contour integration in gestalt perception. We tested the rule of good continuation by stimulating behaving monkeys with simple figures composed of Gabor patches, while recording from upper layer cells in visual cortex (V1). By decomposing these figures into their components and stimulating receptive field centers and surrounds separately with this stimulus set, we tested center-surround interaction for linearity. In pure-fixation tasks, the interaction was negative for the early strong evoked response, i.e., in this phase figural context rather inhibited the cells. However, in the following tonic response phase, a subgroup of neurons showed positive interaction during the whole stimulus presentation period of at least 1000 ms. Attention to the figure in discrimination tasks only slightly improved this positive interaction between 150 and 300 ms. We interpret these results as selective cooperation and mutual facilitation of cortical V1 cells, thereby supporting the saliency of borders and contours in perception of visual scenes.

Keywords Visual cortex · Pattern perception · Binding effects · Monkey

Introduction

Contour integration, image segmentation, and grouping of elements in a scene are considered as basic brain functions in pattern discrimination and gestalt perception. Such operations must work beyond the mechanisms of the classic receptive fields (cRFs), and it seems plausible to assume that they use and integrate cRFs to construct continuous neuronal representations of borders and contours, in other words, that they solve the binding problem. Such integration mechanisms must be fast and flexible, i.e., they should depend neither on time-consuming learning nor on rigid and deterministic wiring. The search for mechanisms with such properties is one of the main efforts of current brain research. Different psychophysical experiments have established rules of how the arrangement of local elements in a visual structure influences the detectability of this structure. Recently several groups of experimenters made use of Gabor patches to construct simple patterns such as lines, curves, or closed figures on a blank or noisy background of similar microstructures (Field et al. 1993; Kovács and Julesz 1993, 1994; Polat and Sagi 1994, 1999; Hess et al. 1998). They found that the detectability of these patterns depends on the distance and relative collinearity of their constituting elements. From these results they concluded that neighboring microstructures influence and amplify each other for higher detectability.

The details of this amplification, which can be considered at least as part of the coding and binding problem at the neuronal level, are still poorly understood. Different, partly controversial concepts have been proposed. They differ with regard to the coding parameter of the relevant neuronal representations, whether they favor a rate code based on single neurons (Rolls 1984; Newsome et al. 1989) or a temporal code (Eckhorn et al. 1990; Singer 1993), or the presence of both parametric aspects in conditioned cell assemblies (Abeles 1982; Braitenberg and Schuez 1991). All such concepts can be generalized as representing different forms and principles of cortical self-organization during perception. We have proposed as a hypothesis our own variant of such cortical self-organization and have simulated its dynamics (Bauer 1993; Bauer and Dicke 1997). The key concept of this hypothesis is a fast, mutual selection of the cells best activated during stimulation, the central element in this process being pyramidal cells, with their two types of excitatory inputs: the driving input from the sensory periphery and the weaker input from neighboring cells via axon collaterals (Hirsch and Gilbert 1991). These two functionally different inputs constitute an elementary, fast

R. Bauer (✉) · S. Heinze
FB Physik/Neurophysik, Philipps-Universität, Renthof 7,
35032 Marburg, Germany
e-mail: Roman.Bauer@physik.uni-marburg.de
Tel.: +49-6421-2824181
Fax: +49-6421-2827034

cooperation system at the cellular level, working by iterative mutual facilitation and selection of coactivated cells.

The use of microstructures such as Gabor patches is of particular advantage for studies of contour integration at the cortical level in two respects. First, size and distance of the figural elements can be scaled to the requirements of the functional anatomy of primary visual cortex (V1). At foveal and parafoveal positions, two cells approximately 2 mm apart in tangential cortical distance have nonoverlapping RFs, but they are still within the reach of their axon collaterals (Dow et al. 1981; Le Vay 1988). Second, line patterns or figures constructed from Gabor patches can be easily decomposed into their components. These can be used as stimuli to measure the effect of stimulating RF centers and surrounds separately, thereby testing wether the stimulus components summate linearly or nonlinearly to the entire figure response. So we chose these stimuli to test the aforementioned psychophysical results (Field et al. 1993; Polat and Sagi 1999) at the neuronal level and to see wether the results would fit the rationale of our hypothesis (Bauer and Dicke 1997). We did this in both pure-fixation and fixation-plus-discrimination tasks to study the contribution of attention in this form of figure perception. According to the classic notion of neuropsychic relations, higher detectability of a figure should be caused by higher firing rates in the stimulated neuronal substrate. Thus, neighboring Gabor patches as local stimuli on a figural path should induce mutual amplification of the stimulated cells in the cortical substrate. We therefore expected that somewhere in the peristimulus-time histogram (PSTH) during stimulation with the entire figure the activity of a cell should be higher than the sum of the responses to both stimulus components. Here we report such cooperativity in pure-fixation and in discrimination tasks. A short version with preliminery results has been published in abstract form (Heinze and Bauer 1999).

Methods

General procedure

Experimental procedures were mainly the same as described in a previous report (Eckhorn et al. 1993b). Two male monkeys (*Macaca mulatta*) were trained to fixate a small light spot during stimulus presentation. Visual stimuli were generated on a computer screen at a frame rate of 94 Hz. In the pure-fixation paradigm, the monkey had to fixate a small spot, ignoring the stimulus, and to release the lever when the fixation spot dimmed. In the discrimination paradigm, the monkey had to fixate the central spot and to decide whether there was a figural pattern on the screen. In this case the monkey had to indicate perception of the figure by down-moving the lever to get a reward. In case there was no figure, he had to release the lever for being rewarded. After monkeys had reached performance rates above 90%, chambers (8 mm o.d.) were screwed to the skull under deep anesthesia, centered to foveal or parafoveal visual field representation (1–2.5° of eccentricity) of V1 in two hemispheres, while leaving the dura intact. All experimental and training procedures were approved and controlled by an official German animal care and use committee, and they followed the guidelines in *Principles of Laboratory Animal Care* (NIH publication No. 86–23, revised 1985).

Stimulus generation and presentation

The stimuli presented to the animals were characterized by separate parameters for: (1) individual elements, (2) positioning of these elements along the figural path, and (3) positioning of the background elements. The single elements were constructed by sinusoidal gratings multiplied by a circular Gaussian function and had a maximal luminance contrast of 40%. The figural path along which the elements were aligned was defined by the distance and the preferred orientations of two separate RF clusters from which we tried to isolate single cells. After the figural path had been determined, the background elements were added to the scene. For this purpose, the screen was divided into a grid. One element was added to each square of this grid unless the square already contained an element of the path. The orientation of the elements and their position within each square were randomly distributed. The spacing of the grid could be adjusted to achieve different task difficulties. Figure 1B shows the three typical stimuli by which each cell was tested: the complete figure (*F*), the figure with the Gabor patch centered on the RF removed (gap stimulus, *G*), and a single Gabor patch centered on the RF (*S*). The spatial extent of a single Gabor patch was less than 0.5° of visual angle, it was adjusted to the size of the cRF center, and the single elements on the figural path were separated by at least one patch size.

Signal recording

Generally we used an array of seven hexagonally arranged microfiber electrodes (spacing 2 mm) which were separately protruded through the intact dura. After recording the first activity, we advanced the electrodes 200–300 μm further so that all recordings were from supragranular layers. We then determined the positions of clustered cRFs at each electrode simultaneously, using the cinematogram method (Eckhorn et al. 1993a). This reverse-correlation technique assigns each recorded cell response to the previous position of a stimulus spot in the visual field. The stimulus is a bright spot with Gaussian luminance profile, jumping randomly in a two-dimensional hexagonal array. The averages of local responses define the spatial extent of the cRF. Figure 1A shows typical RF shapes (70% isoresponse contours). In the next step, we measured the preferred orientation of each RF cluster with light bars presented in eight orientations and moved in 16 directions. Eye position and correct fixation were monitored by means of an infrared reflex photoelectric device. Precision of fixation had to be within ±0.6° of visual angle, otherwise the trial was discarded. Single units were isolated from multiunit activity at each electrode with a multispike detector (MSD; Alpha Omega Engineering) using an on-line template-matching algorithm. We additionally used an adjustable Schmitt trigger for spike detection.

Cooperativity index

This index tests a linear superposition approach: $F=S+G$ with F being the response to the entire figure, and S and G being the responses to the single Gabor patch and the gap stimulus, respectively. We chose the ratio $F:(S+G)-1$ as a hard linearity criterion. A value of zero signifies strict linear summation of the stimulus components S and G in producing the figure response; positive values are interpreted as cooperative enhancement, negative values as inhibition. We called this index the cooperativity index (CI) because the interaction should be strictly mutual between all coactivated cells in neighboring columns. It has been shown that different periods in the peristimulus response of a cell are differentially sensitive to spatial or temporal variations in the stimulus (Richmond et al. 1990; Rolls and Tovee 1994; Motter 1993; Lamme 1995; Lamme et al. 1999; Roelfsema et al. 1998),

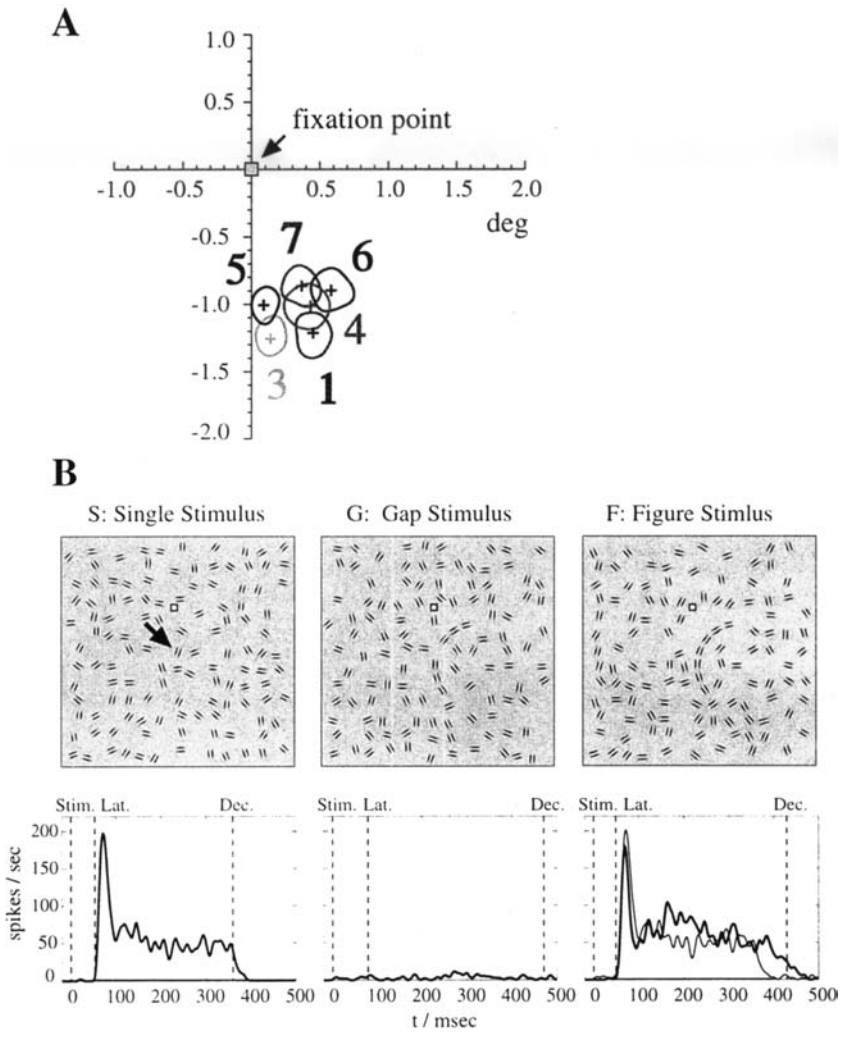

Fig. 1 Stimulation and recording protocol. **A** Visuotopic position, size, and relative distance of six receptive fields obtained with a hexagonal array of seven electrodes. **B** The stimulus triplet with which each cell was tested: *S,* Single patch stimulus centered on the receptive field (*arrow*); *G,* gap stimulus sparing the receptive field; and *F,* entire figure stimulus. *Below* are the corresponding PSTHs summated from 40 single stimulus presentations. *Vertical dashed lines:* first, stimulus onset (*Stim.*); second, cell response onset (*Lat.*); third, earliest decision of the monkey (*Dec.*)

representing different stages of processing. We therefore calculated the CI for successive time windows of 30 ms, beginning from the onset of the response. Thus, the CI was calculated in the following way: (1) determining onset latencies from PSTHs of figure and component responses; (2) dividing the single-unit activities into successive time windows of 30 ms, starting at the defined latency; and (3) calculating the ratio for every time window in each trial. We then obtained the CI as the mean of these ratios across all trials, giving us one CI value for each time window of each cell. Each stimulus type *F*, *S,* and *G*, was tested with 25–40 presentations in randomized sequence.

Latencies and significance tests

Response latencies were defined as the time between stimulus onset and the first detectable response of a given cell. They were quantified as follows: (1) calculating the PSTH; (2) smoothing the PSTH by convolution with a Gaussian function; and (3) application of the latency criterion: increase in activity above mean background activity plus 3 SD. To test the linear superposition approach ($F=S+G$), a Mann-Whitney test ($P<0.05$) was performed for each cell and each time window as an unconditional test. Single-unit activities were preprocessed analogously to steps 1 and 2 in the calculation of CI values.

Results

We tested 266 cells in the upper layers of V1 under comparable conditions with the complete stimulus triplet in both monkeys, 75 cells in pure-fixation tasks and 191 cells in discrimination tasks. Figure 1A shows the size, position, and relative distance of a typical set of RFs that we obtained from the hexagonal array of seven electrodes. Figure 1B shows, below the stimulus set, examples of the corresponding PSTHs from a single cell. In discrimination tasks, stimulus *G* and *F* were perceived and discriminated as figures, while stimulus *S* was not (see Methods). Note that between 150 and 250 ms after stimulus onset, the figure response exceeds the sum of the two component responses (Fig. 1B, thin line in F), pointing to their nonlinear or facilitating interaction in the generation of the figure response.

Cooperativity in fixation task

To analyze these modulation effects systematically in the total population of all cells, we determined the CI.

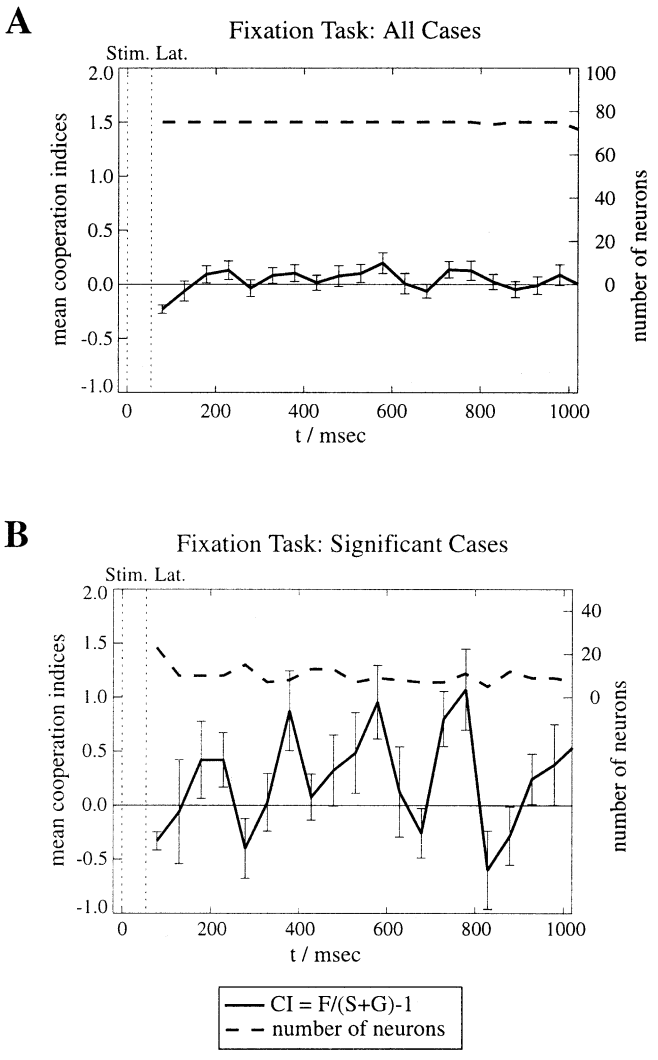

Fig. 2 Results from pure-fixation task. **A** Mean cooperation indices from all cells as a function of stimulus presentation time. **B** Development of significant positive and negative cooperation indices during the same time interval. *Vertical bars,* standard errors of the mean; *dashed lines*, see Fig. 1

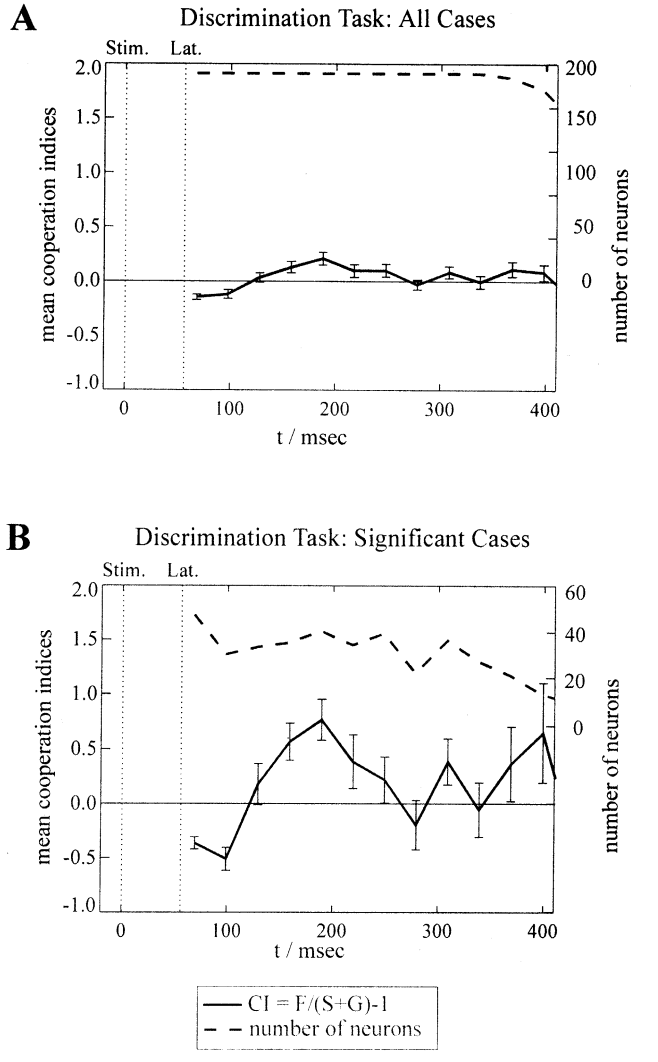

Fig. 3 Results from discrimination task. **A** Mean cooperation indices from all cells as a function of stimulus presentation time. **B** Development of significant positive and negative index values over the same time interval. Same conventions as in Fig. 2

Figure 2A presents the mean CIs from all cells (n=75) during the pure-fixation task on a time scale of 1,000 ms, corresponding to the shortest stimulus presentation times in this task. All values are included: positive and negative, significant and insignificant; thus they fluctuate arround zero, but trends can be seen. Mean CIs were negative during the strong transient cell response following stimulus onset, meaning that during this period the entire stimulus was less effective in driving the cells than the sum of single patch and gap stimulus, probably due to inhibitory influences from the RF surround. Then, however, mean values became positive, indicating that the sign of interaction was reversed. These positive values develop, endure, and fluctuate over the full length of stimulus presentation with periods of 150–200 ms.

The summated CIs in Fig. 2A may contain a subpopulation of cells displaying the modulation effects more clearly than the rest of the sample. We therefore selected those cells whose summated component responses were significantly different (either larger or smaller) from the figural response. Figure 2B shows the respective data from the fixation task on the same scale. Here again CIs are strongly negative during the initial transient cell responses. After that, they fluctuate and oscillate in the positive range, reaching peak values of 100%. The number of cells contributing to the population responses fluctuates over time and is reduced toward the end of the stimulation time, because, when a cell is silent in a time window, the index is not defined and the cell cannot be counted (see CI formula, in the section Cooperativity index). The probability of such cases increases toward the end of the PSTH (see Fig. 1B). For the same reason we calculated the CI index only after the cells' response onset. The number of significant cells can fluctuate even

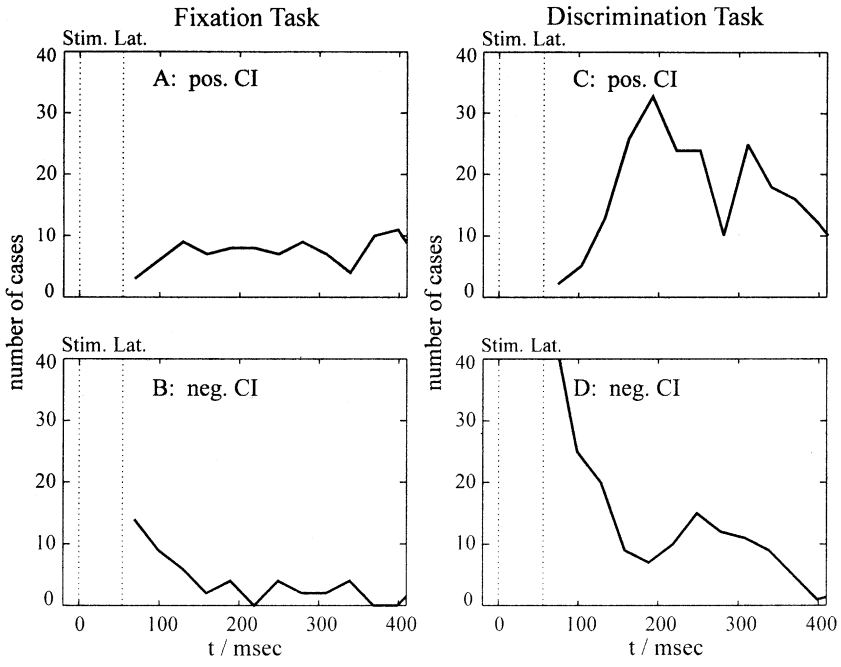

Fig. 4 Frequencies of significant positive and negative cooperation indices (CI) in bins of 30 ms as a function of stimulation time. **A** Proportions of cases with positive and **B** with negative significant cooperation indices in pure-fixation task. **C, D** Proportions of cases with positive (**C**) and with negative (**D**) significant cooperation indices in the discrimination task

more, because a cell can be part of the significant data group in one window but not in the next.

Cooperativity in the discrimination task

Figure 3 shows the corresponding CIs from the discrimination task using the same conventions as in Fig. 2, but with the time axis reduced to 400 ms, which was approximately the earliest reaction time of the monkeys. Figure 3A again presents values from the total cell population (n=191) and Fig. 3B values from the significant cases. The general results are similar to those of Fig. 2, including the fluctuations, but in the early response phase between 100 and 300 ms more CI values are in the positive range than in later phases. This raises the question of the role of attention under the present conditions. On the whole, in each time window in both tasks 15–25% of the cells showed significant (P<0.05) contextual modulation of their firing rates of up to 100% when the figure was present in the stimulus.

Additional role and influence of attention

The periodic CI fluctuations in Figs. 2 and 3 are a robust property of the related neuronal interaction. They appear in both monkeys, and we therefore combined the two data sets without losing the periodic feature. Close inspection of Figs. 2 and 3 reveals more positive CIs between 100 and 300 ms in the discrimination task (Fig. 3) compared with the fixation task (Fig. 2). So far we have presented results from cell populations containing combinations of both positive and negative values of CIs. We therefore separated the significant positive and negative values in a further step. Figure 4A, B show the results from the pure-fixation task and Fig. 4C, D from the discrimination task. During the strong evoked response around 80 ms, negative values dominate in both experimental paradigms. Afterwards, between 150 and 250 ms at the beginning of the steady response, this state is reversed in favor of positive values, with the two time courses having complementary profiles. Between 150 and 250 ms, the relative increase in positive CI values is somewhat stronger in the discrimination task (Fig. 4C, D) than in the fixation task. Although not significant, this small effect could signify a further increase in positive modulation of cell activity by attention.

Latencies of neuronal and behavioral responses

Latencies represent the internal conduction and processing times from stimulus onset to neuronal response or behavioral reaction. Figure 5 presents the mean latencies of neuronal responses. As a criterion for the response onset, we took the time when the activity exceeded the level of resting discharge (which was mostly low and near zero) by 3 SD. In the cases of fast transient responses with the single Gabor patch or the entire figure as stimuli, latencies were short, with little variability around 55 ms. However, when the gap stimulus was delivered, latencies were significantly larger, with mean values around 81 ms. Here, the absence of the fast transient response (see Fig. 1B) is the cause for these prolonged latencies, and these in turn signify that the remaining elements of the gap stimulus did not invade the RF center, but were confined to the surround and to the RFs of cells in neighboring columns, which was a prerequisite of our linearity tests. Typical individual reaction times in the

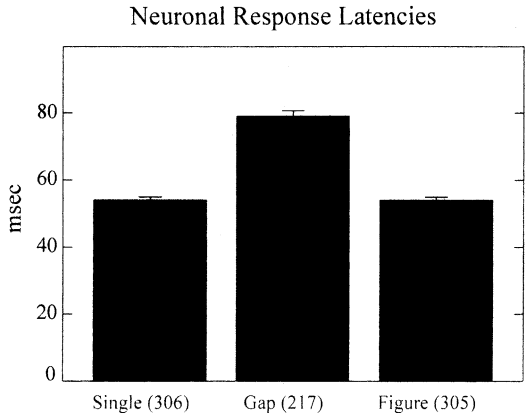

Fig. 5 Mean response latencies from all cells relative to stimulus onset for the three different stimulus conditions (single patch, gap and figure stimulus) from both fixation and discrimination tasks

discrimination task are shown in Fig. 1B. One monkey had much longer reaction times (approimately 1,100 ms) in no-figure discriminations. But apart from this deviation as an individual strategy, all other reaction times in the discrimination task in both monkeys were between 350 and 650 ms, with a mean of 510 ms. They concur with the results from comparable discrimination experiments in the literature (Motter 1993).

We found weak γ-oscillations of local field potentials only late in the fixation task after 500 ms, i.e., at a time, when in the discrimination task the monkey had already decided, and they were not specific for the figure stimulus. However, in a few cases (30) we simultaneously recorded from two cells with RFs separated on the figural path by two Gabor patches. We tested such pairs of cells for spike synchrony in discrimination and fixation tasks. We found a specific short increase in spike coincidences above chance level only when the monkey detected the figure, and these increased coincidences occurred just before or around the monkey's behavioral response (Bauer and Heinze 2002).

Discussion

Psychophysics has established rules of contour integration for gestalt perception such as the rule of good continuation, according to which the proper relative arrangement of local elements in a scene facilitates the integration of those elements into a contour. On recordings from striate cortical cells in trained monkeys, we first performed a strict linearity test in a figural discrimination task and found a neuronal correlate that is probably involved in such enhanced detectability and in the binding of discrete elements into a continuous line or a figure. It is a robust effect appearing reliably in two different task conditions, and it endures over the full time of stimulus presentation of at least 1,000 ms (Fig. 2).

Correlating cell activity and behavior in awake animals has its costs as well as its benefits. Thus, several details of our methods may be confronted with reservation. Control of eye positon and characterization of cell type cannot be accomplished as precisely as with anesthetized animals. Residual eye movements, e.g., could have defeated a clear separation of center and surround stimulation by the figural components. But if so, the gap stimulus should sometimes have evoked strong transient on-responses. This was almost never observed, which is documented by the small standard error of the mean (SEM) of response latencies (see Figs. 1B and 5). For similar reasons, casual eye movements cannot be the cause of the activity fluctuations which were phase-locked to the stimulus and probably induced as theta-waves by the thalamocortical interplay (Miller 1991). They should have been cancelled out by averaging across trials in the same animal and between both animals. Spectral analysis of our data revealed an amplitude peak at 5 Hz in the theta range.

Could our effects have been caused by length summation of the stimulus in a subgroup of cells which were selected by our procedure? The early transient response shows length inhibition rather than summation, indicated by the negative index. Accordingly, in the classic terminology, they would be end-stopped or hypercomplex cells. In the later steady response, in contrast, the response yields positive index values. The conventional classification of cells established on the basis of anesthetized animals may, therefore, not be appropriate to characterize the full temporal dynamic of cells in behavioral tests during contour integration. We found the modulation effect in a small group of approximately 20% in upper layer cells, but they may represent a larger number. Because the succumbing collateral structure is very patchy (Le Vay 1988), the strength of the effect strongly depends on the precise position of the stimulus elements in the center and in the surround of the RFs. Surely these conditions were not satisfied in many cases because of our statistical approach to stimulation and data sampling.

Our present results must be discussed in relation to experiments of other groups in terms of similarities and dissimilarities (Lamme 1995; Lamme et al. 1999; Peterhans and von der Heydt 1989; De Ward et al. 1995; Zipser et al. 1996; Kapadia et al. 1995, 2000; Ito and Gilber 1999; Polat et al. 1998; Knierim and van Essen 1992). These and the present work can be considered as different variants of filling-in effects or as cases of activity modulation by a stimulus in the near or far RF-surround. Lamme (1995) and Zipser et al. (1996) have compared two different global stimuli which were locally identical and symmetrical at the RF site, but different and asymmetrical in the nearer or farther RF surround. One of their stimuli had poor or no contrast in the surround, the other had sharp contrast borders, constituting a closed figure in which contrast-induced activity was captured like in a trap. Other studies used single lines as flanks of the classic RF (Kapadia et al. 1995, 2000; Ito and Gilbert 1999; Polat et al. 1998) or textured patterns (Knierim and van Essen 1992) to test the contextual influence on the

RF. However, there was no spontaneous perceptual integration of a figure in these stimuli. They all found modulatory responses, but they differ in their signs and in temporal delays. Some found strong facilitatory modulation without measurable delay (Kapadia et al. 1995, 2000; Ito and Gilbert 1999), whereas in other experiments contextual modulation was delayed by 100–200 ms (Lamme 1995; Zipser et al. 1996). Inhibition dominated the measurements of Knierim and van Essen (1992), and inhibition or facilitation were found in experiments of Polat et al. (1998) depending on the contrast of the stimulus. Thus, the details of modulation effects seem to be strongly influenced by the experimental circumstances.

Our procedure and our results differ from these studies in several respects. We tested one simple figure and compared its effect with that of its components, thereby testing the linearity or nonlinearity of their cooperation. Furthermore, the elements of our figures were confined to the units of functional anatomy, i.e., to the extent and columnar spacing of local RFs. This correspondence of figural geometry and anatomical structure and the direct comparability with the corresponding psychophysical tests (Field et al. 1993; Kovács and Julesz 1993, 1994; Polat and Sagi 1999) simplifies the functional interpretation of our results. Both effects, the early negative modulation and the reversal to positive modulation at approximately 120 ms after stimulus onset most probably represent different states of information processing within the local cortical network. We interpret the early negative CI values as a classic effect of inhibition by the figural context in the RF surround (see Allman et al. 1985). However, the later, long-lasting positive modulation seems to be a nonclassic effect mediated by the surrounding network of coactivated cells. Its latency and temporal dynamics are compatible with intraareal as well as with interareal connections.

Lamme (1995) and Zipser et al. (1996) stress feedback mechanisms from higher cortical areas as a possible cause of late modulation effects. We prefer to explain these phenomena as being the result of fast, cooperative selection, corresponding to our model and working hypothesis (Bauer 1993; Bauer and Dicke 1997). Accordingly, neurons in columns that are stimulated by neighboring Gabor patches exchange signals reciprocally via their axon collaterals. This fast process can be repeated several times in 100 ms, the most-stimulated cells amplify each other proportionally, thereby promoting themselves as winners, and in this way the most effective connections are selected out of the hardwired plexus. This mechanism operates simultaneously along the total figural path, and so the figure is represented in striate cortex already between 150 and 250 ms by a pattern of prominent activity in a subpopulation of pyramidal cells. Our CI values, their time course, and their dynamics fit into this scheme, and therefore we favor this explanation of late modulation effects.

The contribution of attention still deserves a short comment. The first appearance of activity modulation by attention in the retinocortical information stream has been controversial up to now. It has been commonly held that the first effects of enhanced activity show up at higher levels in extrastriate, but not in striate cortex (see Ito and Gilbert 1999; Martinez et al. 1999; Gilbert et al. 2000). Attention is not an all-or-nothing event, but covers a range of effects from weak to strong activity modulation. In well or overtrained animals, as ours were, an additional amplification by attention may be rather mild. Recent studies using combined event-related potential (ERP) and functional magnetic resonance imaging (fMRI) techniques (Martinez et al. 1999) have provided evidence that V1 is involved in spatial attention. However, according to this study, the earliest modulatory effects of attention do not appear in the short-latency C1 component of the ERP in V1 at 55 ms, but in extrastriate visual areas after 70–75 ms. Only after that can the attention effect also be found in striate cortex, probably due to the top-down flow of a gain control signal (Hupé et al. 1998). Our findings concerning a weak contribution of attention to cooperativity between 150 and 250 ms (Fig. 4) are compatible with these results from the combined ERP and fMRI experiments. In our tests for spike synchrony, however, a strong effect of attention was found (Bauer and Heinze 2002). In summary, our results suggest that the later tonic response in the PSTH of a cell represents a more specific and intriguing phase of information processing and feature representation than the rather unspecific early, fast, and strong evoked response.

Acknowledgements This article was rejected by several journals. We therefore are very grateful to the editors of Experimental Brain Research for fair reviews. We thank Reinhard Eckhorn for providing many laboratory facilities, and W. Gerber and U. Thomas for technical assistance. We are grateful to Reinhard Eckhorn, Michael Brosch, Peter Dicke, and Andreas Bruns for reading the manuscript and for helpful comments and corrections. This work was supported by DFG-grant Ba 636/1,2.

References

Abeles M (1982) Local cortical circuits. Springer, Berlin Heidelberg New York

Allman IM, Meizin F, McGuiness E (1985) Stimulus specific responses from beyond the classical receptive field: neurophysiological mechanisms for local-global comparisons in visual neurons. Annu Rev Neurosci 8:407–430

Bauer R (1993) Selektion – ein Schlüsselbegriff für die strukturelle und funktionelle Selbstorganisation des Gehirns? Naturwissenschaften 80:108–115

Bauer R, Dicke P (1997) Fast cortical selection: a priciple of neuronal self-organization for perception? Biol Cybern 77:207–215

Bauer R, Heinze S (2002) Inter-cellular spike coincidences in visual detection tasks. Naturwissenschaften 89:316–318

Braitenberg V, Schuez A (1991) Anatomy of the cortex. Springer, Berlin Heidelberg New York

De Ward P, Gattas R, Desimone R, Ungerleider LG (1995) Responses of cells in monkey visual cortex during perceptual filling-in of an artificial scotoma. Nature 377:731–734

Dow B M, Snyder A Z, Vautin R G, Bauer R (1981) Magnification factor and receptive field size in foveal striate cortex of the monkey. Exp Brain Res 44:213–228

Eckhorn R, Reitboeck HJ, Arndt M, Dicke P (1990) Feature linking via synchronization among distributed assemblies: simulations of results from cat visual cortex. Neural Comp 2:293–307

Eckhorn R, Krause F, Nelson JI (1993a) The RF-cinematogram. A cross-correlation technique for mapping several visual fields at once. Biol Cybern 63:37–55

Eckhorn R, Frien A, Bauer R, Woelbern T, Kehr H (1993b) High frequency (60–90 Hz) oscillations in primary visual cortex of awake monkey. Neuroreport 4:243–246

Field DJ, Hayes A, Hess RF (1993) Contour integration by the human visual system: evidence for a local "association field". Vision Res 33:173–193

Gilbert CD, Ito M, Kapadia M, Westheimer G (2000) Interaction between attention, context and learning in primary visual cortex. Vision Res 40:1217–1226

Heinze S, Bauer R (1999) Cooperativity between striate cortical cells in the behaving monkey. In: Elsner N, Eysel U (eds) Goettingen Neurobiology Report. Thieme, Stuttgart

Hess RF, Dakin STC, Field DJ (1998) The role of "contrast enhancement" in the detection and appearance of visual contours. Vision Res 38:783–787

Hirsch JA, Gilbert CD (1991) Synaptic physiology of horizontal connections in cat's visual cortex. J Neurosci 11:1800–1809

Hupé JM, James AC, Payne BR, Lombe SG, Girard P, Bullier J (1998) Cortical feedback improves discrimination between figure and background by V1, V2, and V3 neurons. Nature 394:784–787

Ito M, Gilbert CD (1999) Attention modulates contextual influences in the primary visual cortex of alert monkeys. Neuron 22:593–604

Kapadia MK, Ito M, Gilbert CD, Westheimer G (1995) Improvement in visual sensitivity by changes in local context: parallel studies in human observers and in V1 of alert monkeys. Neuron 15:843–856

Kapadia M K, Westheimer G, Gilbert CD (2000) Spatial distribution of contextual interactions in primary visual cortex and in visual perception. J Neurophysiol 84:2084–2062

Kovács I, Julesz B (1993) A closed curve is mutch more than an incomplete one: effect of closure in figure-ground segmentation. Proc Natl Acad Sci USA 90:7495–7497

Kovács I, Julesz B (1994) Perceptual sensitivity maps within globally defined visual shapes. Nature 370:644–646

Knierim JJ, Essen DC van (1992) Neuronal responses to static texture patterns in area V1 of the alert macaque monkey. J Neurophysiol 67:961–980

Lamme VAF (1995) The neurophysiology of figure-ground segregation in primary visual cortex. J Neurosci 15:1605–1615

Lamme VAF, Rodriguez V, Spekreijse H (1999) Separate processing dynamics for texture elements, boundaries and surfaches in primary visual cortex of the macaque monkey. Cereb Cortex 9:406–413

Le Vay S (1988) The patchy intrinsic projections of visual cortex. Prog Brain Res 75:147–161

Martinez A, Anllo-Vento L, Sereno MI, Frank LR, Buxton RB, Dubowitz DJ, Wong EC, Hinrichs H, Heinze HJ, Hillyard SA (1999) Involvement of striate and extrastriate visual cortical areas in spatial attention. Nat Neurosci 2:364–369

Miller R (1991) Cortico-hippocampal interplay and the representation of contexts in the brain. (Studies of brain function, vol 17) Springer, Berlin Heidelberg New York

Motter BC (1993) Focal attention produces spatially selective processing in visual cortical areas V1, V2, and V4 in the presence of competing stimuli. J Neurophysiol 70:909–919

Newsome WT, Britten KH, Mowshon JA (1989) Neuronal correlates of a perceptual decision. Nature 341:52–54

Peterhans E, Heydt R von der (1989) Mechanisms of contour perception in monkey visual cortex. II. Contours bridging gaps. J Neurosci 9:1749–1763

Polat U, Sagi D (1994) The architecture of perceptual spatial interactions. Vision Res 34:73–78

Polat U, Sagi D (1999) Spatial interaction in human vision: from near to far via experience-dependent cascades of connections. Proc Natl Acad Sci USA 91:1206–1209

Polat U, Mizobe K, Pettet MW, Kasamatsu T, Norcia AM (1998) Collinear stimuli regulate visual responses depending on cell's contrast threshold. Nature 391:580–584

Richmond BJ, Optican LM, Spitzer H (1990) Temporal encoding of two-dimensional patterns by single units in primate primary visual cortex. I Stimulus-response relations. J Neurophysiol 64:351–380

Roelfsema PR, Lamme VAF (1998) Object based attention in primary visual cortex of the macaque monkey. Nature 395:376–381

Rolls ET (1984) Neurons in the cortex of the temporal lobe and in the amygdala of the monkey with responses selective for faces. Hum Neurobiol 3:209–222

Rolls ET, Tovee MJ (1994) Processing speed in the cerebral cortex and the neurophysiology of visual masking. Proc R Soc Lond B Biol Sci 257:9–15

Singer W (1993) Synchronization of cortical activity and its putative role in information processing and learning. Annu Rev Physiol 55:349–374

Zipser K, Lamme VAF, Schiller PH (1996) Context modulation in primary visual cortex. J Neurosci 16:7376–7389